

RESEARCH ARTICLE

Dominant effect of gap junction communication in wound-induced calcium-wave, NFAT activation and wound closure in keratinocytes

Laura Hudson¹  | Malcolm Begg²  | Blythe Wright¹  | Tim Cheek³  |
Colin A. B. Jahoda⁴  | Nick J. Reynolds^{1,5} 

¹Institute of Translational and Clinical Medicine, Medical School, Newcastle University, Newcastle upon Tyne, UK

²Medicines Research Centre, GlaxoSmithKline, London, UK

³Biosciences Institute, Medical School, Newcastle University, Newcastle upon Tyne, UK

⁴Department of Biosciences, Durham University, Durham, UK

⁵Department of Dermatology, Royal Victoria Infirmary and NIHR Newcastle Biomedical Research Centre, Newcastle Hospitals NHS Foundation Trust, Newcastle upon Tyne, UK

Correspondence

Nick J. Reynolds, Institute of Translational and Clinical Medicine, Medical School, Newcastle University, Newcastle upon Tyne, UK.

Email: nick.reynolds@newcastle.ac.uk

Funding information

NIHR Biomedical Research Centre, Grant/Award Numbers: BRC_1215_20001, newbrc_2012_1; MRC, Grant/Award Number: Studentship

Abstract

Wounding induces a calcium wave and disrupts the calcium gradient across the epidermis but mechanisms mediating calcium and downstream signalling, and longer-term wound healing responses are incompletely understood. As expected, live-cell confocal imaging of Fluo-4-loaded normal human keratinocytes showed an immediate increase in $[Ca^{2+}]_i$ at the wound edge that spread as a calcium wave (8.3 $\mu\text{m/s}$) away from the wound edge with gradually diminishing rate of rise and amplitude. The amplitude and area under the curve of $[Ca^{2+}]_i$ flux was increased in high (1.2 mM) $[Ca^{2+}]_o$ media. 18 α -glycyrrhetic acid (18 α GA), a gap-junction inhibitor or hexokinase, an ATP scavenger, blocked the wound-induced calcium wave, dependent in part on $[Ca^{2+}]_o$. Wounding in a high $[Ca^{2+}]_o$ increased nuclear factor of activated T-cells (NFAT) but not NF κ B activation, assessed by dual-luciferase receptor assays compared to unwounded cells. Treatment with 18 α GA or the store-operated channel blocker GSK-7975A inhibited wound-induced NFAT activation, whereas treatment with hexokinase did not. Real-time cell migration analysis, measuring wound closure rates over 24 h, revealed that 18 α GA essentially blocked wound closure whereas hexokinase and GSK-7975A showed relatively minimal effects. Together these data indicate that while both gap-junction communication and ATP release from damaged cells are important in regulating the wound-induced calcium wave, long-term transcriptional and functional responses are dominantly regulated by gap-junction communication.

KEYWORDS

ATP signalling, calcium flux, store-operated-calcium-entry

This is an open access article under the terms of the Creative Commons Attribution License, which permits use, distribution and reproduction in any medium, provided the original work is properly cited.

© 2021 The Authors. *Journal of Cellular Physiology* Published by Wiley Periodicals LLC

1 | INTRODUCTION

Tight spatial and temporal regulation of intracellular calcium ($[Ca^{2+}]_i$) signalling allows this ion to control a wide variety of physiological responses including cell growth and differentiation. A steep vertical calcium gradient exists within the epidermis with calcium concentration being low in the proliferative basal layer, progressively increasing through the spinous layer reaching a maximum in the granular layer; levels then fall at the outermost stratum corneum (Elias et al., 2002). Experiments in a wide variety of organisms and cell types have shown that wounding leads to an immediate rise in cytosolic calcium at the wound edge which is followed by a calcium wave radiating away from the site of injury and passing from cell to cell (Tran et al., 1999; Tu et al., 2019). In contrast to excitable cells, wound-induced calcium waves in keratinocytes decay and gradually diminish over relatively short distances (Kobayashi et al., 2014). The wound-induced rapid elevation in $[Ca^{2+}]_i$ and subsequent calcium wave have been shown to be crucial for the downstream calcium-dependent signalling pathways that promote wound closure and organism survival (Tu et al., 2019; Xu & Chisholm, 2011). During wounding of the skin, the epidermal barrier is breached, the dermis is damaged and the wounded tissue is exposed to serum which contains a high concentration of calcium (Bandyopadhyay et al., 2006). However, measurement of wound fluid immediately after cutaneous excisional wounding of pigs showed a reduction of calcium concentration compared to plasma, possibly due to Ca^{2+} sequestration (Grzesiak & Pierschbacher, 1995). A progressive increase in calcium concentration was noted at the incisional skin wound site up to Day 5 in rats (Lansdown et al., 1999). Together, these studies underscore the importance of extracellular calcium to cutaneous wound healing.

Cytosolic increases of calcium can arise essentially from extracellular influx through plasma membrane ion channels, entry of calcium from adjacent cells through gap junctions or $[Ca^{2+}]_i$ release from intracellular stores. The latter occurs primarily from the endoplasmic reticulum (ER), although the Golgi apparatus (Xue et al., 1994) and the mitochondria (De Stefani et al., 2011) have also been reported to be major calcium stores. Calcium release from the ER is primarily triggered by local increases of the soluble mediator inositol 1,4,5-trisphosphate (IP_3) binding to its receptor on the ER and activating Ca^{2+} release through the IP_3 receptor's intrinsic Ca^{2+} channel. Although both calcium and IP_3 may pass through gap junctions (Boitano et al., 1992; Saez et al., 1989), the diffusibility of calcium is relatively limited, due in part to its propensity to interact with a variety of proteins. IP_3 transfer with subsequent triggering of Ca^{2+} release from the ER in adjacent cells is the more likely scenario (Leybaert & Sanderson, 2012), including in keratinocytes (Kobayashi et al., 2014). Depletion of calcium from the ER is sensed by stromal interaction molecule 1 (STIM1) resulting in the translocation of STIM1 to the plasma membrane, activation of calcium release-activate calcium channel protein 1 (Orai1) and subsequent entry of external calcium through Orai1 channels (Stathopoulos et al., 2013). This process, termed store-operated calcium entry (SOCE), inextricably links external calcium concentrations to intracellular calcium fluxes and regulation of cellular processes. Consequently, intra and extracellular calcium sensing proteins play key roles tightly regulating in these signalling pathways by activation of positive

and negative feedback loops (Bird & Putney, 2018; Kobayashi et al., 2014).

Although wound healing is an evolutionary conserved process, the mechanisms contributing to the wound-induced calcium wave vary among organisms and cell types. In keratinocytes, gap junction signalling and release, followed by diffusion of ATP to adjacent cells, where it binds to G protein coupled receptors activating phospholipase C and generating IP_3 , have both been shown to play a role in mediating the wound-induced $[Ca^{2+}]_i$ wave (Karvonen et al., 2000; Kobayashi et al., 2014). Recent studies have also identified a role for the calcium-sensing receptor in mediating the wound-induced calcium flux and the migratory response of keratinocytes (Tu et al., 2019). However, the interplay and relative contribution of ATP signalling, gap junctions and extracellular calcium influx to the generation and propagation of the calcium wave in human keratinocytes is incompletely understood. Moreover, the mechanisms linking calcium signalling occurring in the seconds and minutes after injury to activation of physiological processes required for wound healing remain to be fully defined. IP_3 -mediated SOCE signalling cascade is fundamental to nuclear factor of activated T-cells (NFAT) 1–4 activation and all four calcium-dependent family members are expressed in keratinocytes. In keratinocytes, calcineurin accompanies NFAT1 to the nucleus where it retains NFAT in a dephosphorylated state and therefore NFAT remains nuclear (Al-Daraji et al., 2002). We and other investigators have previously reported that inhibition of calcineurin/NFAT signalling inhibits keratinocyte migration and scratch wound closure (Brun et al., 2014; Jans et al., 2013). In this study, we aimed to analyse specific parameters of the wound-induced calcium wave in human keratinocytes and to delineate pharmacologically the contribution of extracellular ATP signalling, gap-junctional communication, and extracellular calcium influx to further understand the mechanisms of wave transmission. Finally, we designed experiments to establish the relative effects of gap-junctional communication, extracellular ATP and SOCE on both wound-induced NFAT transcriptional activation and keratinocyte migration to close the wound.

2 | MATERIALS AND METHODS

2.1 | Reagents

All chemicals were purchased from Sigma-Aldrich unless otherwise specified.

2.2 | Cell culture and treatments

Normal human epidermal keratinocytes were isolated from normally discarded healthy adult skin samples from patients undergoing a surgical procedure (Jans et al., 2013; Todd & Reynolds, 1998) and expanded in human keratinocyte growth supplement medium (Invitrogen). The study was approved by the Newcastle and North Tyneside local ethics committee, and written informed patient consent was obtained. Keratinocytes were used between Passage 1 and 3.

2.3 | $[Ca^{2+}]_i$ imaging

Keratinocytes seeded in Willco glass-bottomed dishes (Intracel) were loaded with 3 μ M Fluo4-AM, 200 mM sulphapyrazone and 0.1% pluronic acid F-127 and subjected to Ca^{2+}_i imaging using Fluo-4-AM (Invitrogen) as described (Ross et al., 2007). Post-de-esterification, media was replaced with fresh media with a calcium concentration of either 0.06 or 1.2 mM for 5 min before wounding. Single scratch wounds were made approximately 30 s after imaging commenced using a 200 μ l pipette tip. After 20 min, 3 μ M thapsigargin (Tg) was added as a positive control. Imaging was carried out using a Nikon spinning disc TIRF system (Nikon UK Limited) with 20 \times 1.2 lens and excitation wavelength 488 nm. Live images were captured at 3.7 frames per second (fps). Quantification was performed using Volocity (Improvision).

2.4 | ATP release postwounding

ATP release from keratinocytes postwounding was detected using the luminescence-based Cell-titre glo assay (Promega UK).

2.5 | NFAT transcriptional activity assay

NFAT transcriptional activity was measured using an NFAT firefly luciferase reporter plasmid (pGL3; Promega), containing nine copies of an NFAT-binding site from the IL-4 promoter (5'-TGGAAAATT-3') positioned 5' to a minimal promoter from the α -myosin heavy-chain gene, gratefully obtained from J Molckentin, Cincinnati (Wilkins et al., 2004). Transfection efficiency and cell viability were controlled by cotransfecting a *Renilla* luciferase control vector (pRLTK; Promega). Keratinocytes were seeded in 12-well plates and transfected using 0.5 μ g of firefly reporter DNA plus 0.05 μ g of *Renilla* luciferase DNA using Fugene 6 (Roche Applied Sciences) at a 6:1 Fugene:DNA ratio. After 24 h, the cells were stimulated as indicated, lysed, and assayed for dual luciferase activity. Luciferase assays were performed using the dual luciferase assay system (Promega). Reporter firefly luciferase values were normalized to the *Renilla* values.

2.6 | Wound closure rates

A 200 μ l pipette tip was used to create a "cross hatch" wound, on confluent keratinocytes seeded in 24-well plates. Cells were imaged using the Nikon Biostation CT (Nikon UK Limited). ImageJ was used to manually measure the initial wound area and then the subsequent wound area at specified time points.

2.7 | Statistical analysis

Statistical analysis was conducted using Prism (GraphPad 5 or 6 software). Data presented represent mean \pm standard error of the mean

(SEM). N depicts the number of independent donors and n indicates the total number of independent experiments (culture dishes) or number of cells analysed (as specified).

3 | RESULTS

3.1 | Characterisation of wound-induced calcium wave transmission

As expected, real time confocal imaging of primary keratinocytes loaded with Fluo4-AM calcium dye showed an increase in intracellular calcium immediately after wounding, initially focussed at the wound edge; this then spread outward through neighbouring cells during the first 10 s (Figure 1a). To characterise the spread of the calcium wave back from the wound edge, maximum F_t/F_0 , defined as the greatest fold change in $[Ca^{2+}]_i$ flux within individual cells was analysed in "rows" according to their location away from the wound edge, designated 1–6, with cell row 1 being the cell at the wound edge. The time to reach maximum F_t/F_0 across the first six cell rows away from the wound edge fit a linear regression model (Figure 1g). Wounding caused a greater increase in maximum F_t/F_0 $[Ca^{2+}]_i$ in cells at the wound edge with a progressive linear decline in F_t/F_0 $[Ca^{2+}]_i$ in cells further back (Figure 1b), with cell rows 4–6 having a significantly reduced maximum F_t/F_0 compared to cell row 1 ($p < .05$), consistent with previous reports of diminishing signals away from the source of mechanical stimulus (Kobayashi et al., 2014). In line with this, analysis of the time for individual cells to reach maximum F_t/F_0 $[Ca^{2+}]_i$ showed that the further back from the wound edge a cell was located, the longer it took, with cells at the wound edge reaching maximum F_t/F_0 $[Ca^{2+}]_i$ in a shorter time compared to cells six cells back (Figure 1g). Next, we calculated area under the curve (AUC) as an integrative measure of wound-induced calcium flux which in 0.06 mM $[Ca^{2+}]_o$ may be considered an approximation to calcium release from the ER. Figure 1c shows that the AUC of $[Ca^{2+}]_i$ flux decreased progressively in a linear manner across cell rows away from the wound edge, consistent with decline in the maximum F_t/F_0 $[Ca^{2+}]_i$ as the calcium wave travelled away from the wound. Figure 1d shows that that the rate of rise of the $[Ca^{2+}]_i$ flux decreased exponentially the further back from the wound the cells were located. Cells at the wound edge had a rate of rise of 0.67 ± 0.23 ($\Delta F_t/F_0/s$) and those six cells back from the wound had a rate of rise of 0.10 ± 0.03 ($\Delta F_t/F_0/s$) ($p < .05$). Overall, our analysis indicates that after wounding, the calcium wave reduces in amplitude, flux and rate of rise as it travels across cells away from the wound edge. The mechanisms for this dampening remain to be formally determined experimentally, but the pattern of response is most consistent with $[Ca^{2+}]_i$ release gradually diminishing as the wave moves away from the wound. This model is compatible with both gap-junction communication and paracrine ATP signalling (Fujii et al., 2017; Kobayashi et al., 2014) and the diminishing ability of IP_3 and/or extracellular ATP to regenerate IP_3 (Sneyd et al., 1995).

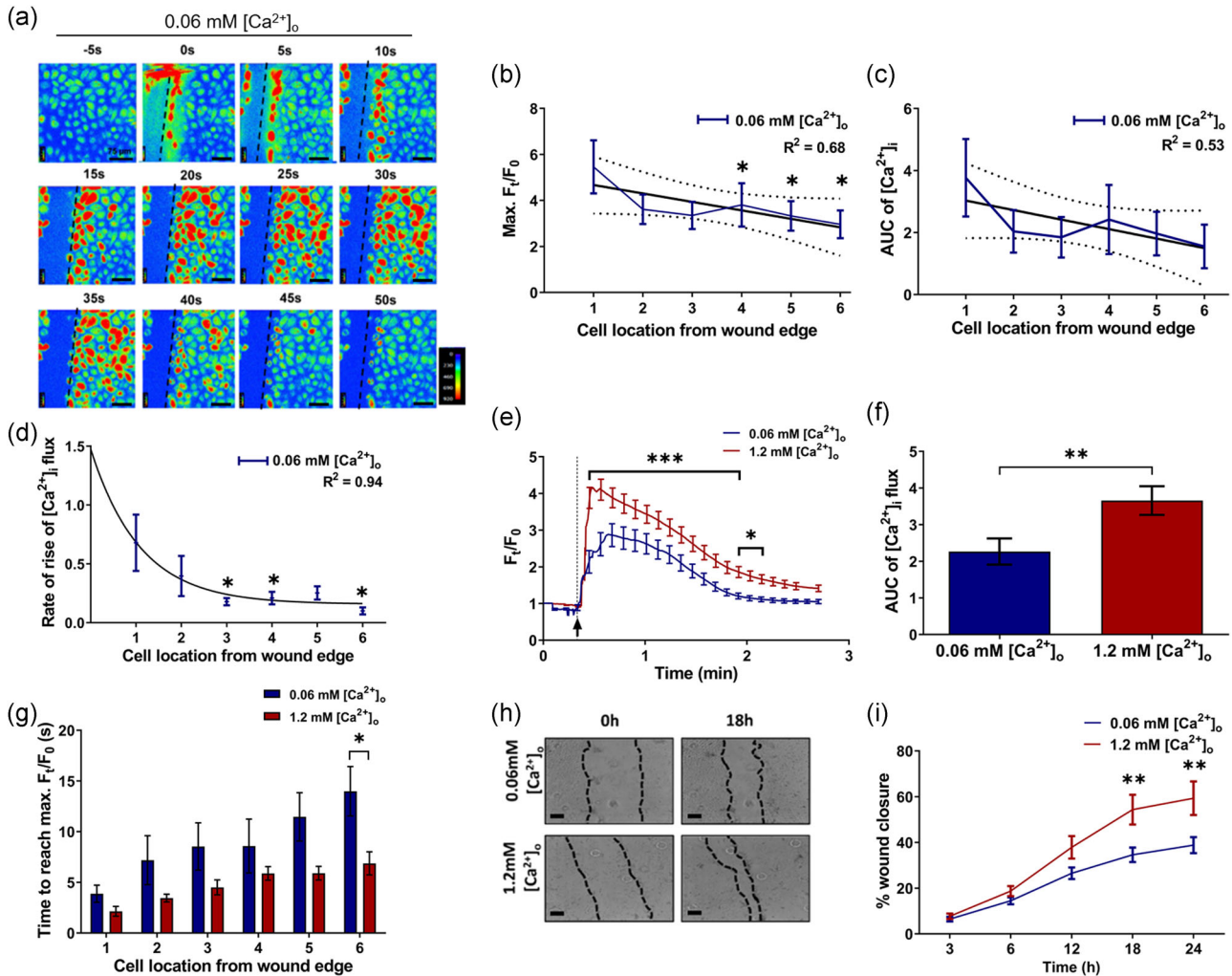


FIGURE 1 Distinct characteristics of wound-induced calcium wave and differential closure rates in low and high extracellular calcium conditions. Primary human keratinocytes cultured in 0.06 mM $[Ca^{2+}]_o$ KGM were loaded with Fluo4-AM calcium dye. Post-de-esterification, either 0.06 mM (a–i) (blue lines/bars) or 1.2 mM $[Ca^{2+}]_o$ (e–i) (red/brown lines/bars) KGM was added for 5 min before scratch wounding. (a) Pseudo colour images of real time confocal images (Scale bar = 80 μ m). Wound edge is highlighted by dotted line. Representative of three independent donors. (b–d; g) Specified parameters were analysed at each cell location from the wound edge. Linear regression line and 95% CI (dotted lines) (b, c, g) and nonlinear regression exponential decay graph (d) are shown. Data represent mean \pm SEM from 12 cells at each location from three independent donors ($n = 72$, $N = 3$). (b) Maximum (max) F_f/F_0 $[Ca^{2+}]_i$ flux. $*p < .05$ compared to cell row 1, one-way ANOVA, Dunnett's post-hoc test. (c) AUC, $p < .0001$ one-way ANOVA, posttest for linear trend. (d) Rate of rise $[Ca^{2+}]_i$ flux, $**p < .01$, $*p < .05$ compared to cell row 1, one-way ANOVA with Dunnett's post-hoc test. (e) F_f/F_0 $[Ca^{2+}]_i$ flux (mean \pm SEM plotted every 7 s for clarity) from 72 cells across rows 1–6 in three independent donors wounded in 0.06 mM (blue) or 1.2 mM (red) $[Ca^{2+}]_o$. $***p < .001$, $*p < .05$, 0.06 mM compared to 1.2 mM $[Ca^{2+}]_o$ at each time point, two-way ANOVA with Bonferroni post-hoc test. (f) AUC (mean \pm SEM) for $[Ca^{2+}]_i$ fluxes in 0.06 mM (blue bar) and 1.2 mM $[Ca^{2+}]_o$ (red bar); $**p < .01$, unpaired T-test ($n = 72$ cells, $N = 3$ donors). (g) Time taken to reach maximum fold change (F_f/F_0) $[Ca^{2+}]_i$ flux in 0.06 mM (blue) or 1.2 mM (red) $[Ca^{2+}]_o$; two-way ANOVA $p < .0001$ and $*p < .05$ Bonferroni post-hoc test 0.06 mM compared to 1.2 mM $[Ca^{2+}]_o$. (h) Representative images taken at predetermined co-ordinates every 1 h for 24 h. Black lines depict wound edge (Scale bar = 250 μ m). (i) Wound size was measured at each time point using Image J and percent of wound closure calculated (mean \pm SEM; 18 experiments from six independent donors; $n = 18$, $N = 6$). Two-way ANOVA $p < .0001$; $**p < .01$ Bonferroni post hoc test between the two external calcium concentrations. ANOVA, analysis of variance; AUC, area under the curve; CI, confidence interval; KGM, keratinocyte growth medium

3.2 | Effect of increased extracellular calcium concentration on wound-induced calcium wave characteristics

Although the overall pattern of the $[Ca^{2+}]_i$ fluxes appeared similar whether keratinocytes were wounded in 0.06 mM or 1.2 mM $[Ca^{2+}]_o$ KGM,

the maximal $[Ca^{2+}]_i$ flux induced by wounding, was significantly larger when wounding was performed in 1.2 mM $[Ca^{2+}]_o$ (Figure 1e). Analysis of cells according to their location from the wound edge, showed no difference in the calcium flux at the wound edge (Figure S1a) between cells cultured in 0.06 mM or 1.2 mM $[Ca^{2+}]_o$. Notably, however, the mean calcium signal (F_f/F_0) and AUC of $[Ca^{2+}]_i$ flux were significantly increased

in cells located two to six rows from the wound, in 1.2 mM $[Ca^{2+}]_o$ compared to 0.06 mM $[Ca^{2+}]_o$ (Figure S1b–f). Additionally, as shown in Figure 1g, the time taken to reach maximum F_i/F_o was reduced when wounding was conducted in 1.2 mM $[Ca^{2+}]_o$. Intriguingly, rate of rise of $[Ca^{2+}]_i$ was the only parameter examined that was not affected by external calcium at cell locations either close to and further back from the wound edge. If rate of $[Ca^{2+}]_i$ rise is taken as an approximation to the rate at which calcium is released from intracellular stores, such as the ER, this supports a model in which IP_3 transfer across cells induces calcium release from the ER which leads to increased calcium entry in 1.2 mM $[Ca^{2+}]_o$ (Boitano et al., 1992).

Based upon the effects of $[Ca^{2+}]_o$ on $[Ca^{2+}]_i$ flux in keratinocytes, we hypothesised that wounding in a high external calcium environment would enhance keratinocyte wound closure. To test this, we performed real time imaging of keratinocytes wounded in 0.06 or 1.2 mM $[Ca^{2+}]_o$ KGM. At earlier time points postwounding (3–6 h), little difference was observed but after 12 h, significantly increased wound closure rates were observed in 1.2 mM compared with 0.06 mM $[Ca^{2+}]_o$ (Figure 1h,i) ($p < .01$).

3.3 | GSK-7975A inhibits SOCE in keratinocytes

GSK-7975A, a pyrazole derivative, is an effective and highly selective SOCE inhibitor that interferes with ion permeation through the Orai1 selectivity pore (Chaudhari et al., 2020; Derler et al., 2013). However, its efficacy in primary keratinocytes has to date, not been reported. To address this, primary human keratinocytes in 1.2 mM $[Ca^{2+}]_o$ KGM were treated with 3 μ M thapsigargin (Tg) to deplete ER calcium stores and initiate SOCE (Figure S2). Real time calcium flux imaging showed that 10 μ M GSK-7975A or 10 μ M diethylstilbestrol (DES) (Jans et al., 2013) blocked SOCE in primary keratinocytes (Figure S2). However, sulforhodamine B (SRB) cell viability assays demonstrated that DES was toxic to primary human keratinocytes at 24 h whereas GSK-7975A did not appear to reduce cell viability. As we were interested in correlating early calcium flux changes with later wound healing responses, we subsequently used GSK-7975A to inhibit SOCE and study its role in wound-induced calcium wave.

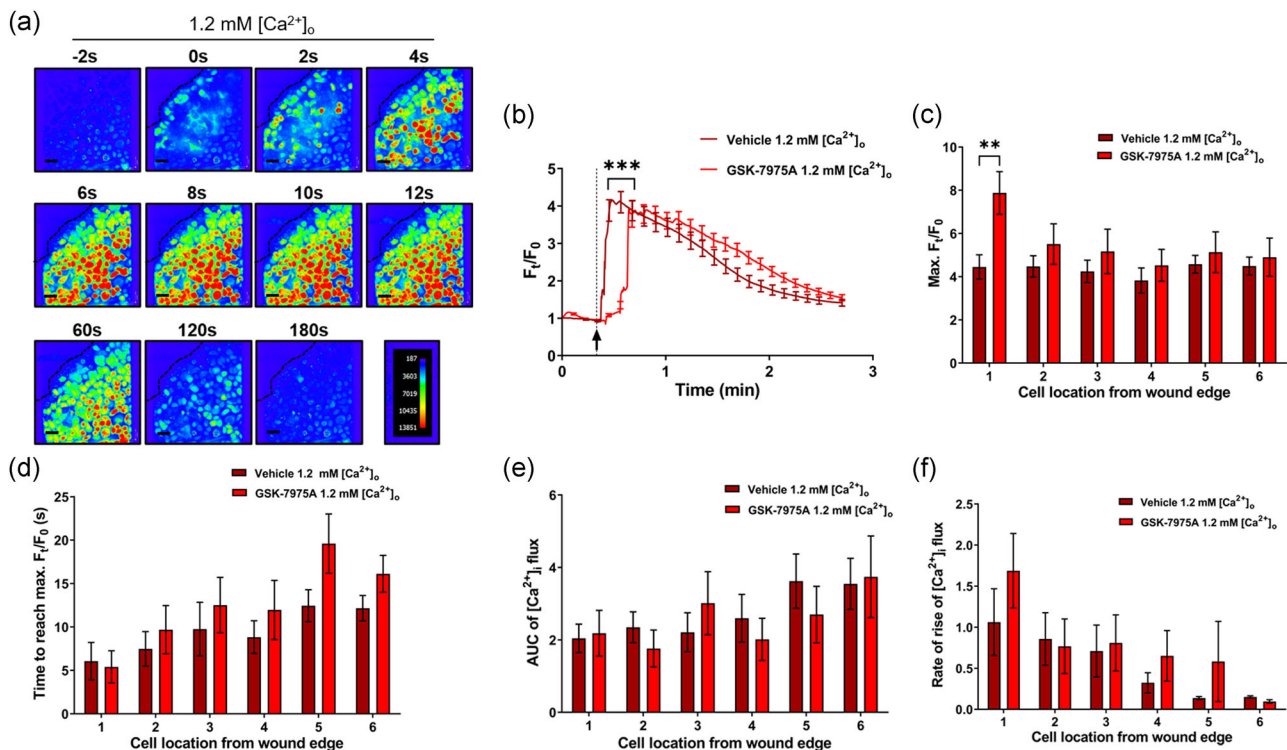


FIGURE 2 Effect of SOCE blockade on wound-induced calcium flux. Primary human keratinocytes loaded with Fluo4-AM calcium dye were treated with 10 μ M GSK-7975A or vehicle in 0.06 mM KGM for 45 min and then 5 min before wounding switched to 0.06 or 1.2 mM $[Ca^{2+}]_o$ KGM with 10 μ M GSK-7975A. (a) Pseudo colour images of confocal images were generated before the wound being made (-2 s), at the point of wounding (0 s) and then at the time points indicated following addition of GSK-7975A in 1.2 mM $[Ca^{2+}]_o$ (Scale bar = 80 μ m). Pseudo colour reference is shown. Wound edge is highlighted by dashed line. Images are representative of three independent donors. (b) F_i/F_o $[Ca^{2+}]_i$ flux from 72 cells across rows 1–6 in three independent donors wounded in 1.2 mM $[Ca^{2+}]_o$ in presence of GSK-7975A or control. *** $p < .001$ two-way ANOVA with Bonferroni post-hoc, GSK-7975A compared to vehicle. (c–e) Specified parameters (mean \pm SEM) from 12 cells at each location ($n = 72$ cells; $N = 3$ donors) were analysed at each cell row location from the wound edge. (C) Maximum (Max) fold change (F_i/F_o) $[Ca^{2+}]_i$ flux. Two-way ANOVA $p = .007$ and ** $p < .01$ Bonferroni post-hoc test GSK-7975A compared to vehicle. (d) Time taken to reach maximum F_i/F_o $[Ca^{2+}]_i$ flux. Two-way ANOVA $p = .04$ GSK-7975A compared to vehicle (e) AUC for $[Ca^{2+}]_i$ fluxes. Two-way ANOVA $p = .16$ GSK-7975A compared to vehicle (f) Rate of rise $[Ca^{2+}]_i$ flux. Two-way ANOVA $p = .14$ GSK-7975A compared to vehicle. ANOVA, analysis of variance; KGM, keratinocyte growth medium; SOCE, store-operated calcium entry

3.4 | Role of SOCE in the wound-induced calcium wave

Keratinocytes wounded in 1.2 mM $[Ca^{2+}]_o$ KGM in the presence of 10 μ M GSK-7975A showed a $[Ca^{2+}]_i$ flux at the wound edge which spread as a wave through neighbouring cells in a broadly similar pattern compared to a vehicle control (Figure 2a). Overall, (and specifically in cells two to six rows back from the wound), blocking SOCE did not significantly affect the wound-induced $[Ca^{2+}]_i$ flux (Figure 2c). The wave took a significantly longer time to reach six cells back from the wound edge when wounds were performed in the presence of GSK-7975A compared to vehicle ($p = .04$, two-way ANOVA), suggesting that SOCE contributes to the speed of propagation of the wound induced calcium wave (Figure 2d). However, blocking SOCE with GSK-7975A, did not significantly affect the AUC or rate of rise of the wound-induced $[Ca^{2+}]_i$ flux (Figure 2e,f). Together, these data provide evidence that SOCE does not affect the overall $[Ca^{2+}]_i$ flux away from the wound edge, consistent with the effects of 1.2 mM $[Ca^{2+}]_i$ compared to 0.06 mM $[Ca^{2+}]_i$ (Figure 1g) although SOCE may enhance the speed of the wound-induced calcium wave. On the other hand and rather unexpectedly, the maximum F_i/F_o $[Ca^{2+}]_i$ flux induced by wounding in 1.2 mM $[Ca^{2+}]_o$ in cells located at the wound edge was significantly increased in the presence of GSK-7975A compared to vehicle (Figure 2c). These data suggest that blocking SOCE channels at the wound edge may release a reciprocal inhibitory mechanism enhancing calcium entry through store independent calcium entry (SICE) channels (Zhang et al., 2018), for example, as previously described (Mignen et al., 2001, 2003). Maximum F_i/F_o and AUC of wound-induced $[Ca^{2+}]_i$ flux were greater in 1.2 mM $[Ca^{2+}]_i$ compared to 0.06 mM $[Ca^{2+}]_i$ (Figure 1e,f) but SOCE inhibition by GSK-7975A did not significantly affect these parameters. These observations implicate activation of SICE channels (Zhang et al., 2018) or may be explained by activation of the calcium sensing receptor (Tu et al., 2019).

3.5 | Role of gap junction communication in mediating the wound-induced calcium wave

In mammalian cells, intercellular calcium wave propagation is thought to occur predominantly through a combination of gap-junction communication and paracrine ATP signalling (Fujii et al., 2017; Kobayashi et al., 2014). Passage of IP_3 through gap-junctions, binding to IP_3R on the ER and further initiation of SOCE has been shown in a variety of cell types. ATP-mediated calcium waves are slower compared to direct gap junctional signalling but can spread between cells either side of a cell-free zone (Frame & de Feijter, 1997) and even across different cell types (Koizumi et al., 2004). ATP released via connexin and pannexins (Bao et al., 2004; Barr et al., 2013) is able to bind to $P2YRs$ on neighbouring cells, activating phospholipase C (PLC) and inducing an IP_3 -mediated release of calcium from the ER and subsequently SOCE. However, there is a lack of consensus regarding the relative contribution of each pathway in mediating calcium signal transmission in keratinocytes (Korkiamaki

et al., 2005; Tsutsumi et al., 2009). We therefore sought to investigate pharmacologically the role of gap junctions and extracellular signalling on wound induced calcium flux in keratinocytes.

18 α glycyrrhetic acid (18 α GA) (Davidson et al., 1986), a stereo-isomer metabolite of glycyrrhizin, blocks gap junction communication through modification of phosphorylation of residues in the cytoplasmic tail of Connexin 43 (Cx43) leading to changes in the assembly of connexins required for a functional gap-junction (Guan et al., 1996). As Cx43 is the most abundant connexin in mammals and is expressed throughout the epidermis (Martin et al., 2014), and 18 α GA blocks dye transfer across gap-junction in keratinocytes (Easton et al., 2019), we utilised 18 α GA to investigate the relative contribution of gap-junction communication to wound-induced calcium wave in human keratinocytes.

Figures 3a and 3d show that immediately following wounding in 1.2 mM $[Ca^{2+}]_o$ in the presence of 18 α GA, $[Ca^{2+}]_i$ increased within cells located at the wound edge but to a significantly lesser degree compared to control conditions in 0.06 mM $[Ca^{2+}]_o$ (Figure 1b) and 1.2 mM $[Ca^{2+}]_o$ (Figure 3d). Moreover, in 0.06 mM $[Ca^{2+}]_o$, 18 α GA substantially and significantly reduced the overall $[Ca^{2+}]_i$ flux compared to control (Figure 3b) resulting in a marked and significantly diminished maximum fold change (F_i/F_o) (Figure 3d) and AUC of $[Ca^{2+}]_i$ flux (Figure 3h) at all specified locations from the wound edge. Additionally, as shown by Figure 3f, 18 α GA treatment in 0.06 mM $[Ca^{2+}]_o$ had an overall delaying effect on the time taken to reach maximum F_i/F_o ($p = .0007$, two-way ANOVA) which was most pronounced two rows back from the wound edge ($p < .05$, Bonferroni post-hoc), consistent with a more rapid spread of the calcium wave through gap junctions (compared to ATP paracrine effects).

Wounding in the presence of 18 α GA in 1.2 mM $[Ca^{2+}]_o$ caused a reduced maximum F_i/F_o and AUC of $[Ca^{2+}]_i$ flux compared to vehicle in cells at all specified locations from the wound edge, although in contrast to experiments in 0.06 mM $[Ca^{2+}]_o$ the difference was more notable at locations distal to the wound (Figures 3e and 3i).

However, again in contrast to experiments in 0.06 mM $[Ca^{2+}]_o$, 18 α GA had no significant effect on the time to reach maximum $[Ca^{2+}]_i$ following wounding in 1.2 mM $[Ca^{2+}]_o$ (Figure 3g).

Together these data provide evidence that blockade of gap-junction communication significantly abrogates the transduction of $[Ca^{2+}]_i$ signal initiated at the wound edge. Interestingly, however, wounding in the presence of 18 α GA in 1.2 mM $[Ca^{2+}]_o$, reduced parameters of the wave but not to the extent observed in 0.06 mM $[Ca^{2+}]_o$ (Figure 3b,c). Both the maximum F_i/F_o reached and AUC of the wound-induced $[Ca^{2+}]_i$ flux were not significantly diminished by 18 α GA in 1.2 mM $[Ca^{2+}]_o$ compared to vehicle within cells located at the wound edge; however both maximum F_i/F_o reached and AUC then decreased with increasing location from the wound edge (Figures 3e and 3i). These data suggest that other mechanisms, including for example calcium entry potentially combined with extracellular ATP signalling, could partially overcome blockade of gap junctions close to the wound edge and enable partial transduction of the calcium wave.

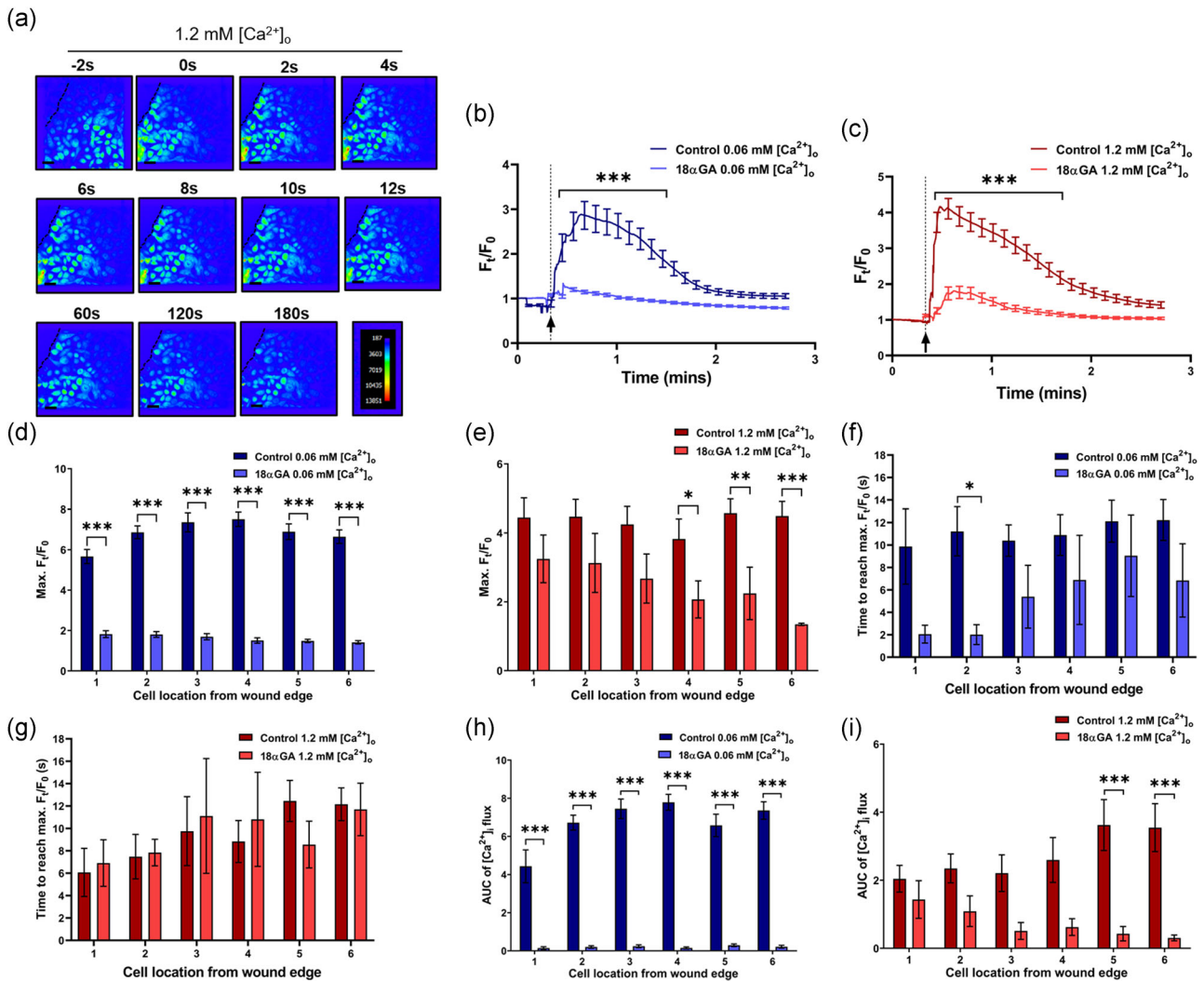


FIGURE 3 Abrogation of wound-induced intercellular calcium wave by 18 α GA in both low and high external calcium conditions. Primary human keratinocytes loaded with Fluo4-AM calcium dye were treated with 20 μ M 18 α GA or vehicle in 0.06 mM KGM for 45 min and then 5 min before wounding switched to 0.06 mM or 1.2 mM $[Ca^{2+}]_o$ KGM with 20 μ M 18 α GA. (a) Pseudo colour images of confocal images were generated before the wound being made (-2 s), at the point of wounding (0 s) and then at the time points indicated following pretreatment with 18 α GA in 1.2 mM $[Ca^{2+}]_o$ KGM (Scale bar = 80 μ m). Pseudo colour reference is shown. Wound edge is highlighted by dotted line. Images are representative of three independent donors. (b) F_t/F_0 $[Ca^{2+}]_i$ flux from 72 cells across rows 1–6 in three independent donors wounded in 0.06 mM $[Ca^{2+}]_o$ in presence of 18 α GA or control. *** p < .001 two-way ANOVA with Bonferroni post-hoc test, 18 α GA compared to control. (c–h) Specified parameters (mean \pm SEM from 12 cells at each location from three independent donors (n = 72; N = 3) were analysed at each cell row location from the wound edge. (c) and (d) Maximum (Max) fold change F_t/F_0 $[Ca^{2+}]_i$ flux in 0.06 mM (c) or 1.2 mM $[Ca^{2+}]_o$ (d) in presence of 18 α GA or control. Two-way ANOVA p < .0001; *** p < .0001, ** p < .01, * p < .05, Bonferroni post-hoc test, 18 α GA compared to control. (e,f) Time taken to reach max F_t/F_0 $[Ca^{2+}]_i$ flux for wounds made 0.06 mM (e) or 1.2 mM $[Ca^{2+}]_o$ (f). Two-way ANOVA p = .0007, * p < .05, bonferroni post-hoc test, 18 α GA compared to control. (g, h) AUC of $[Ca^{2+}]_i$ flux for wounds made 0.06 mM (g) or 1.2 mM $[Ca^{2+}]_o$ (h). Two-way ANOVA p = .0001, *** p < .001, Bonferroni post-hoc test 18 α GA compared to control. 18 α GA, 18 α -Glycyrrhetic acid; ANOVA, analysis of variance; KGM, keratinocyte growth medium

3.6 | Role of extracellular ATP signalling in mediating the wound-induced calcium wave

Addition of wounded conditioned media to unwounded cells triggers a $[Ca^{2+}]_i$ flux in a variety of cell types (Sammak et al., 1997). To determine whether extracellular paracrine factors were playing a role in wound-induced calcium flux, human keratinocytes were scratch wounded in a cross-hatch manner in either 0.06 or 1.2 mM $[Ca^{2+}]_o$. Five minutes postwounding, the conditioned media (CM) was

collected and added to unwounded keratinocytes that had been loaded with the calcium dye Fluo4-AM. Following addition of the CM, $[Ca^{2+}]_i$ flux increased within a subpopulation of cells which remained elevated for several minutes (Figure S3).

Stress or mechanical perturbation results in release of ATP from keratinocytes (Barr et al., 2013; Moehring et al., 2018) and ATP at physiological concentrations causes a calcium response in unwounded cells (Figure S4) in either 0.06 or 1.2 mM $[Ca^{2+}]_o$ (Ross et al., 2007). To confirm that wounding induced ATP release and

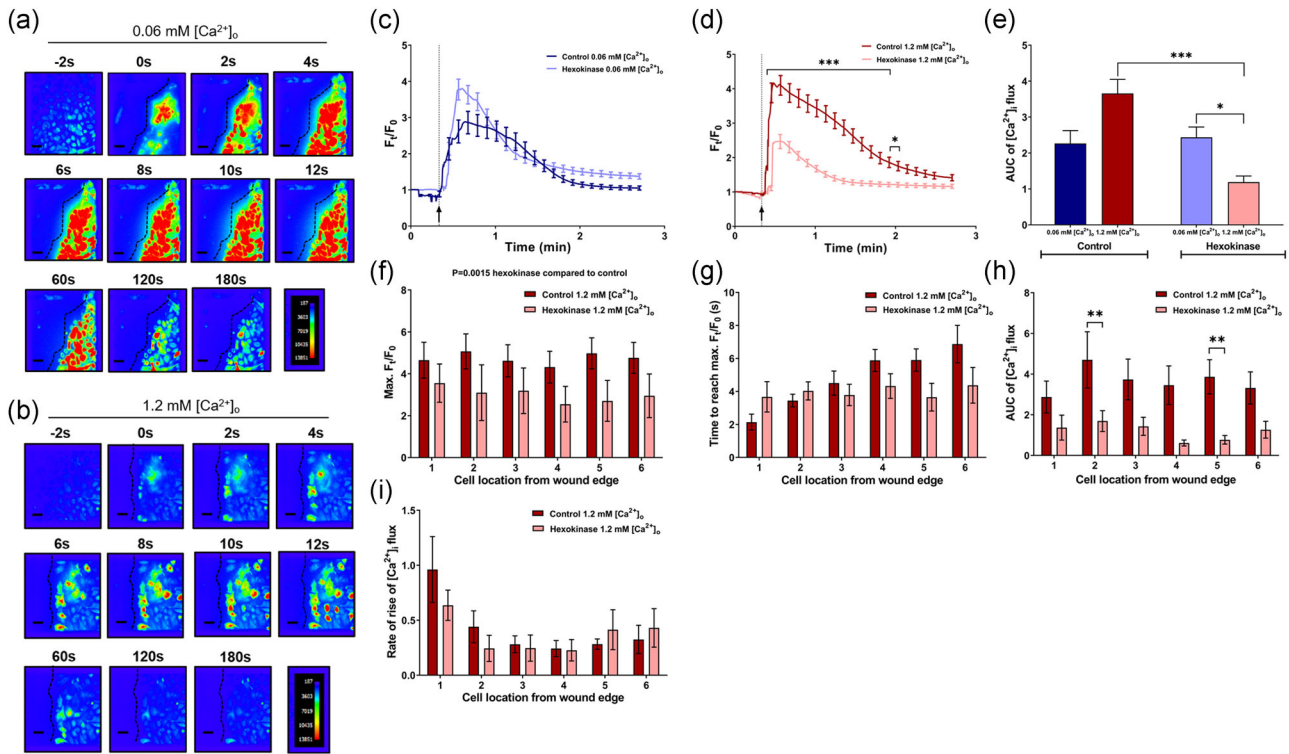


FIGURE 4 Abrogation of wound-induced intercellular calcium wave by hexokinase is dependent on external calcium conditions. Primary human keratinocytes loaded with Fluo4-AM calcium dye were treated with 50 U/ml hexokinase or vehicle for 45 min in 0.06 or 1.2 mM $[Ca^{2+}]_o$ KGM before wounding. (a, b) Pseudo colour images of confocal images were generated before the wound being made (-2 s), at the point of wounding (0 s) and then at the time points indicated in the presence of hexokinase in 0.06 mM (a) or in 1.2 mM $[Ca^{2+}]_o$ (b) KGM (Scale bar = 80 μ m). Pseudo colour reference is shown. Wound edge is highlighted by dotted line. Images are representative of three independent donors. F_f/F_o $[Ca^{2+}]_i$ flux (c) and (d) and AUC $[Ca^{2+}]_i$ flux (e) from 72 cells across rows 1–6 in three independent donors wounded in 0.06 mM (c) or 1.2 mM $[Ca^{2+}]_o$ (d) in presence of hexokinase or control. (c) Two-way ANOVA, $p = .2507$; (d) Two-way ANOVA $p < .0001$; $***p < .001$, $*p < .05$ Bonferroni post-hoc test hexokinase compared to control. (e) Two-way ANOVA $p = .0003$; $***p < .001$, $*p < .05$ Bonferroni post-hoc. (f–i) Specified parameters (mean \pm SEM) from 12 cells at each location from three independent donors; $n = 72$; $N = 3$) were analysed at each cell row location from the wound edge. (f) Max fold change (F_f/F_o) $[Ca^{2+}]_i$ flux in 1.2 mM $[Ca^{2+}]_o$. Two-way ANOVA, $p = .0015$, hexokinase compared to control. (g) Time taken to reach max F_f/F_o $[Ca^{2+}]_i$ flux for wounds made in 1.2 mM $[Ca^{2+}]_o$. Two-way ANOVA $p = .07$, hexokinase compared to control. (h) AUC of $[Ca^{2+}]_i$ flux for wounds made in 1.2 mM $[Ca^{2+}]_o$. Two-way ANOVA $p < .0001$; $**p < .01$, Bonferroni post-hoc test hexokinase compared to control. (i) Rate of rise $[Ca^{2+}]_i$ flux, two-way ANOVA $p = .1786$, hexokinase compared to control. ANOVA, analysis of variance; AUC, area under curve; KGM, keratinocyte growth medium

determine the time course, we measured ATP in the medium following cross hatch wounding. Postwounding, ATP was released from keratinocytes immediately following wounding and persisted in the medium for up to 60 min in both 0.06 mM and 1.2 mM $[Ca^{2+}]_o$ (Figure S5).

To investigate the contribution of ATP release to wound induced $[Ca^{2+}]_i$ flux, we utilised the ATP scavenger hexokinase (Liu et al., 2008) (Cheek et al., 1989) which essentially depleted detectable levels of extracellular ATP in unwounded and wounded samples in either 0.06 or 1.2 mM $[Ca^{2+}]_o$ (Figure S6). Pretreatment of keratinocytes with 50 U/ml hexokinase substantially decreased the intracellular calcium flux and reduced the spread of the calcium wave in 1.2 mM $[Ca^{2+}]_o$ (Figures 4b and 4d) but not 0.06 mM $[Ca^{2+}]_o$ (Figures 4a, 4c, and S7). Moreover, in 0.06 mM $[Ca^{2+}]_o$, hexokinase treatment did not significantly affect the wound-induced $[Ca^{2+}]_i$ flux (F_f/F_o , AUC) overall or at any cell location from the wound edge

(Figures 4a, 4c, and 4e). For wounds performed in 1.2 mM $[Ca^{2+}]_o$, treatment with hexokinase significantly decreased $[Ca^{2+}]_i$ flux (F_f/F_o) compared to control (Figures 4d and 4f). Kinetic analysis showed a reduction in time taken to reach maximum F_f/F_o in cells 5 and 6 rows back from the wound with hexokinase treatment (Figure 4g), consistent with faster transmission of the wave through gap junctions, although this did not reach statistical significance ($p = .07$, two way ANOVA). AUC was also significantly reduced by pretreatment with hexokinase compared to control in 1.2 mM $[Ca^{2+}]_o$ (Figures 4e and 4h), perhaps reflecting reduced ATP-induced calcium entry from the extracellular space. Finally, Figure 4i shows that hexokinase did not influence the rate of rise of the $[Ca^{2+}]_i$ flux induced by wounding which decreased the further back from the wound the cell was located. Together these data show that ATP paracrine signalling significantly contributes to the wound-induced calcium wave in 1.2 mM $[Ca^{2+}]_o$ but seems to play little role in 0.06 mM $[Ca^{2+}]_o$.

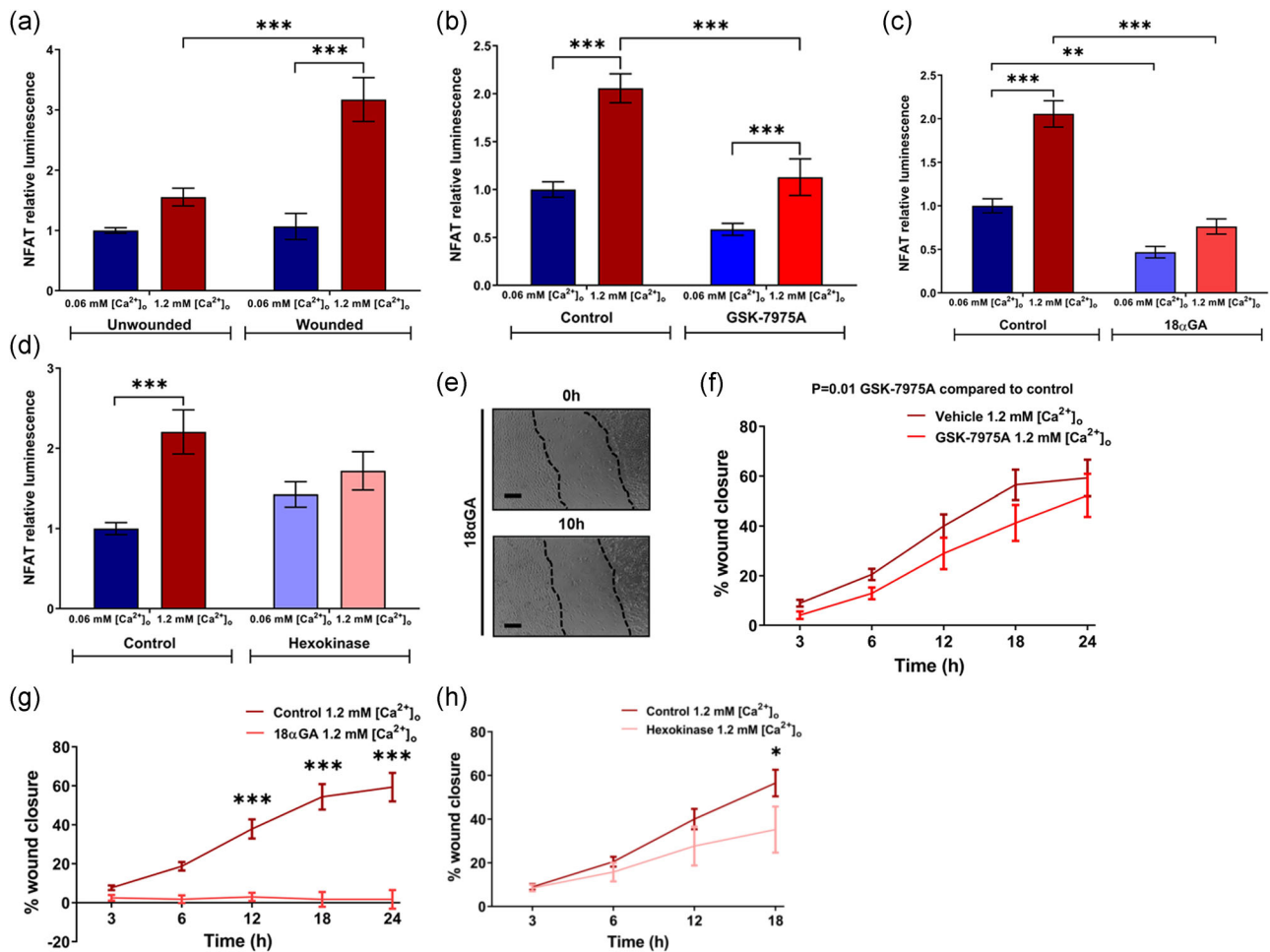


FIGURE 5 Differential effects of SOCE, ATP and gap junction signalling on wound-induced NFAT activation and wound closure in human keratinocytes. (a–d) Primary human keratinocytes cultured in 0.06 mM $[Ca^{2+}]_o$ KGM were transfected with NFAT firefly and renilla luciferase constructs and cultured until 100% confluent. Luciferase activity (mean firefly/renilla ratio \pm SEM normalised to unwounded 0.06 mM $[Ca^{2+}]_o$) was measured 24 h after wounding. (a) Medium was replaced with either 0.06 or 1.2 mM $[Ca^{2+}]_o$ KGM before cross-hatch wounding; 47 experiments from 17 independent donors ($n = 47$, $N = 17$). Two-way ANOVA $p = .0002$; *** $p < .001$ Bonferroni post-hoc. (b) Medium was replaced with either 0.06 or 1.2 mM $[Ca^{2+}]_o$ KGM with 10 μ M GSK-7975A or 1:1000 vehicle (DMSO) for 1 h before cross-hatch wounding ($n = 19$, $N = 7$). Two-way ANOVA $p < .0001$; *** $p < .001$ Bonferroni post-hoc. (c) Medium was replaced with either 0.06 or 1.2 mM $[Ca^{2+}]_o$ KGM with 20 μ M 18 α GA or 1:1000 vehicle (DMSO) for 1 h before cross-hatch wounding ($n = 15$, $N = 5$). Two-way ANOVA $p < .0001$; *** $p < .001$, ** $p < .01$ Bonferroni post-hoc. (d) Medium was replaced with either 0.06 or 1.2 mM $[Ca^{2+}]_o$ KGM with 50 U/ml hexokinase or control for 5 min before cross-hatch wounding ($n = 18$; $N = 6$). Two-way ANOVA, $p = .8802$. (e–h) Primary human keratinocytes cultured in 0.06 mM $[Ca^{2+}]_o$ KGM were grown to confluency and treated with 20 μ M 18 α GA (a, g), 10 μ M GSK-7975A (e) and 50 U/ml hexokinase (h) in 1.2 mM $[Ca^{2+}]_o$ for 1 h before wounding. Images were taken at predetermined co-ordinates every hour for 24 h. (e) Representative images of wound closure. Black lines depict wound edge (Scale bar = 250 μ m). (f–g) Wound area was measured using Image J and calculated as a percentage of the original wound size. Graphs show mean \pm SEM. (f) Two-way ANOVA $p = .01$ comparing wound closure rates between untreated and GSK-7975A treated cells; 10 experiments from three independent donors ($n = 10$, $N = 3$). (g) Two-way ANOVA $p < .0001$; *** $p < .001$ Bonferroni post hoc test comparing wound closure in untreated and 18 α GA treated cells ($n = 9$, $N = 3$). (h) Two-way ANOVA $p = .01$, * $p < .05$ Bonferroni post-hoc test comparing wound closure rates between untreated and hexokinase treated cells ($n = 12$, $N = 4$). 18 α GA, 18 α -Glycyrrhetic acid; ANOVA, analysis of variance; DMSO, dimethyl sulfoxide; KGM, keratinocyte growth medium; NFAT, Nuclear factor of activated T-cell; SOCE, store-operated calcium entry

3.7 | Wound-induced NFAT activation in human keratinocytes

Sustained increases in $[Ca^{2+}]_i$ results in calcium ions binding to calmodulin which in turn activates the serine phosphatase calcineurin. Calcineurin dephosphorylates the calcium dependent factor NFAT (isoforms 1–4), exposing its nuclear localisation domain resulting in

NFAT translocation to the nucleus and transcriptional activation (Hogan et al., 2003). As keratinocytes express all four calcium-dependent NFAT isoforms (Al-Daraji et al., 2002) which are activated by a variety of stimuli (Flockhart et al., 2008) and play a functional role in regulating growth, differentiation and migration (Jans et al., 2013; Wilson et al.), we hypothesised that wounding would activate NFAT in primary human keratinocytes. Moreover, by using

NFAT as a functional readout of wound-induced $[Ca^{2+}]_i$ flux, we aimed to investigate the relative contribution of SOCE, gap junctions and extracellular ATP signalling to wound-induced NFAT activation.

We measured wound-induced NFAT activation, in primary keratinocytes using a NFAT transactivation luciferase assay. Preliminary experiments established that wounding induced maximal increase in NFAT activity at 24 h. Unwounded cells exposed to 1.2 mM $[Ca^{2+}]_o$ showed a small 1.55 ± 0.14 -fold increase in NFAT activation compared to unwounded cells in 0.06 mM $[Ca^{2+}]_o$ (Figure 5a) ($p > .05$). Wounding in 1.2 mM $[Ca^{2+}]_o$ but not in 0.06 mM $[Ca^{2+}]_o$ resulted in a robust activation of NFAT at 24 h (Figure 5a). In contrast, wounding did not activate canonical Nf κ B signalling as determined by luciferase assay in keratinocytes although Nf κ B-dependent luciferase activity was induced by 1.2 mM $[Ca^{2+}]_o$ (Figure S8) consistent with the role of Nf κ B in regulating keratinocyte differentiation (Hinata et al., 2003). These data indicate that a high external calcium environment, is required for NFAT activation postwounding.

3.8 | Relative contribution of SOCE, gap junction communication and extracellular ATP signalling in mediating wound-induced NFAT activation

As wound-induced NFAT activation in keratinocytes required a high calcium external environment, we tested the role of SOCE, by wounding cells in the presence of the SOCE inhibitor GSK7975A or vehicle (dimethyl sulfoxide). Wounding in the presence of GSK-7975A $[Ca^{2+}]_o$ significantly attenuated wound-induced increase in NFAT-dependent luciferase activity in 1.2 mM (Figure 5b). These results support a role for SOCE in mediating wound-induced NFAT activation postwounding.

As blocking gap-junctional communication using 18 α GA significantly reduced wound-induced intracellular calcium flux and prevented the spread of the calcium wave following scratch wounding, we tested whether 18 α GA inhibited wound-induced NFAT activation in 1.2 mM $[Ca^{2+}]_o$. While wounding untreated cells in 0.06 mM $[Ca^{2+}]_o$ did not induce NFAT activity, blocking gap-junctional communication before wounding reduced NFAT activation in low calcium conditions. Furthermore, wounding in the presence of 18 α GA in 1.2 mM $[Ca^{2+}]_o$ completely blocked NFAT activation to below that seen when wounding in 0.06 mM $[Ca^{2+}]_o$ (Figure 5c).

Primary human keratinocytes release ATP immediately after wounding (Figure S4). Moreover, ATP induced intracellular calcium signalling in a subpopulation of unwounded cells (Figure S4). Cells wounded in 1.2 mM $[Ca^{2+}]_o$ following hexokinase treatment showed attenuated elevation of NFAT-dependent luciferase compared to control, but this difference was not statistically significant (Figure 5d).

In summary, these data support the conclusion that wound-induced activation of NFAT in keratinocytes occurs predominantly through SOCE-mediated calcium influx in 1.2 mM $[Ca^{2+}]_o$ and a gap junction-dependent mechanism.

3.9 | Dominance of gap-junction communication in mediating wound closure compared to SOCE and extracellular ATP

Gap-junction inhibition using 18 α GA prevented the spread of the calcium wave postwounding (Figure 3) as well as reducing wound-induced NFAT activation (Figure 5c). We therefore hypothesised that blockade of gap-junctional communication would have a significant functional effect on wound closure. To address this, primary human keratinocytes were pretreated with 20 μ M 18 α GA for 1 h before wounding in KGM with a calcium concentration of either 0.06 or 1.2 mM.

Blocking gap-junctional communication compared to untreated cells wounded in 1.2 mM $[Ca^{2+}]_o$ (Figure 1h), reduced wound closure at all time points following wounding (Figures 5e and 5g) (Two-way ANOVA $p < .0001$); significantly so after 12 h ($p < .001$ Bonferroni post hoc test) resulting in minimal wound closure over 24 h. Similarly, 18 α GA significantly inhibited wound closure in 0.06 mM $[Ca^{2+}]_o$ (Figure S9) compared to control (Figure 1h).

Although blocking SOCE with GSK-7975A, did not significantly affect early wound-induced $[Ca^{2+}]_i$ flux (Figure 2), wounding in the presence of GSK-7975A significantly attenuated wound-induced NFAT activation in 1.2 mM $[Ca^{2+}]_o$ at 24 h (Figure 5b). To investigate whether SOCE inhibition at the point of wounding had a functional effect on wound closure, cells were pretreated with 10 μ M GSK-7975A for 1 h before wounding in 1.2 mM $[Ca^{2+}]_o$. Compared to untreated cells wounded in 1.2 mM $[Ca^{2+}]_o$ (Figure 1h), inhibiting SOCE partially decreased wound closure overall ($p = .01$, two-way ANOVA) (Figure 5f).

ATP is released by keratinocytes upon wounding and removal of ATP by hexokinase in the extracellular media following wounding, significantly reduced the intracellular calcium flux postwounding in 1.2 mM $[Ca^{2+}]_o$ (Figure 4d,e). To test whether removal of extracellular ATP by treatment with hexokinase had a functional effect on cell migration, primary human keratinocytes monolayers were wounded in either 0.06 or 1.2 mM $[Ca^{2+}]_o$ in the presence or absence of 50 U/ml hexokinase. Compared to untreated cells wounded in 1.2 mM $[Ca^{2+}]_o$ (Figure 1h), removal of extracellular ATP increased wound closure at later time points ($p = .0135$, two-way ANOVA) and specifically at 18 h (Figure 5h) ($*p < .05$, Bonferroni post-hoc test). Conversely and perhaps surprisingly, in cells wounded in 0.06 mM $[Ca^{2+}]_o$ it appears that removal of extracellular ATP increased wound closure rates at later time points (two-way ANOVA $p < .0025$) (Figure S10).

Taken together these data showed that keratinocyte migration during wound closure is regulated by SOCE, extracellular ATP and gap-junctional communication. However, blockade of gap-junctional communication exerted the most profound effect, completely prevented wound closure in keratinocytes with relatively small contributions from SOCE and extracellular ATP. In keratinocytes, intercellular communication between cells following wound appears necessary for effective cell migration to close the wound.

3.10 | Concluding remarks

While the roles of extracellular and intracellular calcium regulating keratinocyte growth and differentiation have been well characterised, the mechanisms integrating these signals to regulate cutaneous wound healing are less well understood. Our studies comparing responses in 0.06 and 1.2 mM $[Ca^{2+}]_o$ showed no differences in $[Ca^{2+}]_i$ flux response at the immediate wound edge suggesting that intracellular stores are the principle source for the initiation of the wound-induced wave. On the other hand, in cells further from the wound edge, calcium entry from the extracellular space was a major determinant for the amplitude of wound-induced $[Ca^{2+}]_i$ flux response. Notably, wounds closed significantly faster in 1.2 mM $[Ca^{2+}]_o$ compared to 0.06 mM $[Ca^{2+}]_o$. Interestingly, treatment with the GSK-7975A SOCE inhibitor, which was highly effective at blocking SOCE in keratinocytes, slowed the speed of the wound-induced calcium wave but did not affect the overall $[Ca^{2+}]_i$ flux away from the wound edge. Mechanical wounding is believed to trigger an increase in IP_3 in cells at the wound edge, although exact mechanisms are still not understood and $[Ca^{2+}]_i$ flux at the wound edge was unaffected by $[Ca^{2+}]_o$. GSK-7975A enhanced $[Ca^{2+}]_i$ at the wound edge suggesting that blockade of SOCE enhances SICE in these particular cells.

Removing extracellular ATP, substantially abrogated wound induced $[Ca^{2+}]_i$ in 1.2 mM $[Ca^{2+}]_o$ but had no effect on intracellular calcium flux in 0.06 mM $[Ca^{2+}]_o$. These data suggest therefore, that in a lower calcium extracellular environment, gap junction and IP_3 -mediated mechanisms rather than extracellular signalling predominate in regulating wound induced calcium wave in keratinocytes. On the other hand, in a higher calcium extracellular environment, ATP-mediated influx of calcium from the extracellular space, was required for full propagation of the wave. In considering the relative contribution of gap-junction and paracrine signalling to the spread of the wound-induced intercellular calcium, it is important to note that inhibitors of gap-junctional communication may also decrease ATP release. For example, Cotrina et al. demonstrated that overexpression of Cx43 increased intercellular calcium wave through increased ATP release rather than increased gap-junction signalling (Cotrina et al., 1998). Isakson et al. demonstrated that the mechanical damage-induced $[Ca^{2+}]_i$ wave was not lost in the presence of a gap junction inhibitor but was in the presence of ATPase apyrase (Isakson et al., 2001). Faniku et al. showed that inhibition of Cx43 inhibited ATP release in a concentration-dependant manner in calcium deprivation (Faniku et al., 2018) and Kawano et al. showed in human bone marrow-derived mesenchymal stem cells that $18\alpha GA$ blocked ATP-induced calcium oscillations and NFAT activation (Kawano et al., 2006). Notably though pretreatment of keratinocytes with $18\alpha GA$ did not significantly reduce wound-induced ATP release (Figure S11). Nevertheless, it is likely that ATP release and gap-junction signalling interact synergistically to trigger an intercellular calcium wave, NFAT activation and cell migration. For example, Iacobus et al. demonstrated this by analysing the characteristics of the intercellular calcium wave. These authors showed that wound-induced IP_3 -mediated waves only travelled a short distance, about five cells but combining ATP and

IP_3 signalling mechanisms resulted in a longer propagation distance (Iacobus et al., 2006). In our study, it appears though that signalling through gap junctions was apparently unable to overcome blockade of ATP signalling in 1.2 mM $[Ca^{2+}]_o$, reinforcing a model in which complex feedback loops integrate signals emanating from ATP signalling, calcium entry, and gap junctions.

As SOCE regulates NFATc1 translocation in keratinocytes (Jans et al., 2013) and ciclosporin and RNAi-mediated knockdown of NFATc1 inhibits lysophosphatidic acid-induced keratinocyte migration (Jans et al., 2013), we investigated whether scratch wounding resulted in transcriptional activation of NFAT. Our findings that wounding only activated NFAT in 1.2 mM $[Ca^{2+}]_o$ which was markedly attenuated by GSK-7975A underscores the role of SOCE in wound-induced NFAT activation. Wounding in the presence of hexokinase did not attenuate transcriptional activity and the addition of ATP at a physiologically relevant concentration to unwounded keratinocytes did not induce NFAT transcriptional activation. Therefore, extracellular ATP released by keratinocytes following wounding does not appear to play a significant role in NFAT activation. This is in contrast to human bone marrow-derived mesenchymal stem cells (hMSCs) in which extracellular ATP released through hemi-gap-junction channels induced spontaneous calcium oscillations and downstream nuclear translocation of NFATc3 (Kawano et al., 2006). Pharmacological inhibition of ATP release prevented induction of the calcium oscillations and blocked nuclear translocation of NFAT (Kawano et al., 2006). However, when these stem cells differentiated into adipocytes both spontaneous oscillations and NFAT activation ceased (Kawano et al., 2006). Similar results were seen in microglial cells in which Ferrari et al. observed that ATP was able to activate NFAT (Ferrari et al., 1999).

The propagation of the calcium wave through the population of cells appears to be important for downstream transcriptional activation, as determined by a reduction in wound-induced NFAT activation when wounding was performed in the presence of $18\alpha GA$. By studying Cx45^{-/-} mice embryos, Kumai et al. showed that signalling through gap-junctions was required to activate NFATc1 (Kumai et al., 2000). In knockout mice compared to wild type embryos, the authors showed that Cx45 regulated nuclear translocation of NFATc1. Consistent with these findings, we found that $18\alpha GA$, significantly inhibited wound induced $[Ca^{2+}]_i$ flux and NFAT transcriptional activation in both low and high external calcium conditions.

Scratch wound closure in 1.2 mM $[Ca^{2+}]_o$ was only marginally reduced by SOCE inhibition and removal of extracellular ATP. Conversely inhibition of gap-junctions robustly prevented cell migration in both 0.06 mM $[Ca^{2+}]_o$ and 1.2 mM and blocked NFAT activation in 1.2 mM $[Ca^{2+}]_o$, providing further evidence that the calcium wave induced by wounding is crucial in long-term functional events.

In summary, while both purinergic and gap-junction signalling regulate the intracellular calcium flux and calcium wave immediately following postwounding, there is a dominant effect of gap-junction communication in the activation of NFAT and cell migration, leading to wound closure over 24 h. Studies to further determine mechanisms regulating each of these pathways in relation to epidermal wound healing and the translation of these findings into a 3D skin

equivalent model, will hopefully lead to the development of novel therapies to enhance wound closure.

ACKNOWLEDGEMENTS

We thank Dr. Anna Brown who helped optimising the conditions for calcium-flux experiments, Professor Fiona Oakley for help and support and Carole Todd for expert technical support. We thank the MRC for funding. The research was also supported by the NIHR Newcastle Biomedical Research Centre. NJR is a NIHR Senior Investigator.

CONFLICT OF INTERESTS

Nick Reynolds has received research grant funding to Newcastle University from Novartis, GSK and PSORT partners (<https://www.PSORT.org.uk>). Malcolm Begg is employed by GSK. The other authors declare no conflicts of interest.

DATA AVAILABILITY STATEMENT

The data generated in the work reported was derived from human samples donated by patients under Biobank ethical and intuitional approval. Any reasonable request for anonymised data access will be met by the authors.

ORCID

Laura Hudson  <http://orcid.org/0000-0003-3403-0569>

Malcolm Begg  <http://orcid.org/0000-0001-9508-3424>

Blythe Wright  <http://orcid.org/0000-0002-0624-2751>

Tim Cheek  <http://orcid.org/0000-0001-8424-2725>

Colin A. B. Jahoda  <http://orcid.org/0000-0002-1762-1220>

Nick J. Reynolds  <http://orcid.org/0000-0002-6484-825X>

REFERENCES

- Al-Daraji, W. I., Grant, K. R., Ryan, K., Saxton, A., & Reynolds, N. J. (2002). Localization of calcineurin/NFAT in human skin and psoriasis and inhibition of calcineurin/NFAT activation in human keratinocytes by cyclosporin A. *The Journal of Investigative Dermatology*, 118(5), 779–788.
- Bandyopadhyay, B., Fan, J., Guan, S., Li, Y., Chen, M., Woodley, D. T., & Li, W. (2006). A “traffic control” role for TGFβ3: Orchestrating dermal and epidermal cell motility during wound healing. *Journal of Cell Biology*, 172(7), 1093–1105.
- Bao, L., Locovei, S., & Dahl, G. (2004). Pannexin membrane channels are mechanosensitive conduits for ATP. *FEBS Letters*, 572(1-3), 65–68.
- Barr, T. P., Albrecht, P. J., Hou, Q., Mongin, A. A., Strichartz, G. R., & Rice, F. L. (2013). Air-stimulated ATP release from keratinocytes occurs through connexin hemichannels. *PLOS One*, 8, 2.
- Bird, G. S., & Putney, J. W., Jr. (2018). Pharmacology of store-operated calcium entry channels. In J. A. Kozak, & J. W. Putney, Jr. (Eds.), *Calcium entry channels in non-excitable cells* (pp. 311–324). CRC Press/Taylor & Francis.
- Boitano, S., Dirksen, E. R., & Sanderson, M. J. (1992). Intercellular propagation of calcium waves mediated by inositol trisphosphate. *Science*, 258(5080), 292–295.
- Brun, C., Demeaux, A., Guaddachi, F., Jean-Louis, F., Oddos, T., Bagot, M., Bensussan, A., Jauliac, S., & Michel, L. (2014). T-plastin expression downstream to the calcineurin/NFAT pathway is involved in keratinocyte migration. *PLOS One*, 9(9), e104700.
- Chaudhari, S., Yazdizadeh Shotorbani, P., Tao, Y., Davis, M. E., Mallet, R. T., & Ma, R. (2020). Inhibition of interleukin-6 on matrix protein production by glomerular mesangial cells and the pathway involved. *American Journal of Physiology. Renal Physiology*, 318(6), F1478–F1488.
- Cheek, T. R., Jackson, T. R., O'Sullivan, A. J., Moreton, R. B., Berridge, M. J., & Burgoyne, R. D. (1989). Simultaneous measurements of cytosolic calcium and secretion in single bovine adrenal chromaffin cells by fluorescent imaging of fura-2 in cocultured cells. *The Journal of Cell Biology*, 109(3), 1219–1227.
- Cotrina, M. L., Lin, J. H. C., Alves-Rodrigues, A., Liu, S., Li, J., Azmi-Ghadimi, H., Kang, J., Naus, C. C. G., & Nedergaard, M. (1998). Connexins regulate calcium signaling by controlling ATP release. *Proceedings of the National Academy of Sciences of the United States of America*, 95(26), 15735–15740.
- Davidson, J. S., Baumgarten, I. M., & Harley, E. H. (1986). Reversible inhibition of intercellular junctional communication by glycyrrhetic acid. *Biochemical and Biophysical Research Communications*, 134(1), 29–36.
- De Stefani, D., Raffaello, A., Teardo, E., Szabó, I., & Rizzuto, R. (2011). A forty-kilodalton protein of the inner membrane is the mitochondrial calcium uniporter. *Nature*, 476(7360), 336–340.
- Derler, I., Schindl, R., Fritsch, R., Heftberger, P., Riedl, M. C., Begg, M., House, D., & Romanin, C. (2013). The action of selective CRAC channel blockers is affected by the Orai pore geometry. *Cell Calcium*, 53(2), 139–151.
- Easton, J. A., Albuloushi, A. K., Kamps, M. A. F., Brouns, G., Broers, J. L. V., Coull, B. J., Oji, V., van Geel, M., van Steensel, M. A. M., & Martin, P. E. (2019). A rare missense mutation in GJB3 (Cx31G45E) is associated with a unique cellular phenotype resulting in necrotic cell death. *Experimental Dermatology*, 28(10), 1106–1113.
- Elias, P. M., Ahn, S. K., Denda, M., Brown, B. E., Crumrine, D., Kimutai, L. K., Kömüves, L., Lee, S. H., & Feingold, K. R. (2002). Modulations in epidermal calcium regulate the expression of differentiation-specific markers. *Journal of Investigative Dermatology*, 119(5), 1128–1136.
- Faniku, C., O'Shaughnessy, E., Lorraine, C., Johnstone, S. R., Graham, A., Greenhough, S., & Martin, P. E. M. (2018). The connexin mimetic peptide Gap27 and Cx43-knockdown reveal differential roles for Connexin43 in wound closure events in skin model systems. *International Journal of Molecular Sciences*, 19(2).
- Ferrari, D., Stroh, C., & Schulze-Osthoff, K. (1999). P2X7/P2Z purinoreceptor-mediated activation of transcription factor NFAT in microglial cells. *The Journal of Biological Chemistry*, 274(19), 13205–13210.
- Flockhart, R. J., Duffey, B. L., Farr, P. M., Lloyd, J., & Reynolds, N. J. (2008). NFAT regulates induction of COX-2 and apoptosis of keratinocytes in response to ultraviolet radiation exposure. *The FASEB Journal*, 22(12), 4218–4227.
- Frame, M. K., & de Feijter, A. W. (1997). Propagation of mechanically induced intercellular calcium waves via gap junctions and ATP receptors in rat liver epithelial cells. *Experimental Cell Research*, 230(2), 197–207.
- Fujii, Y., Maekawa, S., & Morita, M. (2017). Astrocyte calcium waves propagate proximally by gap junction and distally by extracellular diffusion of ATP released from volume-regulated anion channels. *Scientific Reports*, 7(1), 13115.
- Grzesiak, J. J., & Pierschbacher, M. D. (1995). Shifts in the concentrations of magnesium and calcium in early porcine and rat wound fluids activate the cell migratory response. *The Journal of Clinical Investigation*, 95(1), 227–233.
- Guan, X., Wilson, S., Schlender, K. K., & Ruch, R. J. (1996). Gap-junction disassembly and connexin 43 dephosphorylation induced by 18 beta-glycyrrhetic acid. *Molecular Carcinogenesis*, 16(3), 157–164.
- Hinata, K., Gervin, A. M., Jennifer Zhang, Y., & Khavari, P. A. (2003). Divergent gene regulation and growth effects by NF-kappa B in

- epithelial and mesenchymal cells of human skin. *Oncogene*, 22(13), 1955–1964.
- Hogan, P. G., Chen, L., Nardone, J., & Rao, A. (2003). Transcriptional regulation by calcium, calcineurin, and NFAT. *Genes & Development*, 17(18), 2205–2232.
- Iacobas, D. A., Suadicani, S. O., Spray, D. C., & Scemes, E. (2006). A stochastic two-dimensional model of intercellular Ca²⁺ wave spread in glia. *Biophysical Journal*, 90(1), 24–41.
- Isakson, B. E., Evans, W. H., & Boitano, S. (2001). Intercellular Ca²⁺ signaling in alveolar epithelial cells through gap junctions and by extracellular ATP. *American Journal of Physiology Lung Cellular and Molecular Physiology*, 280(2), L221–L228.
- Jans, R., Mottram, L., Johnson, D. L., Brown, A. M., Sikkink, S., Ross, K., & Reynolds, N. J. (2013). Lysophosphatidic acid promotes cell migration through STIM1- and Orai1-mediated Ca²⁺ mobilization and NFAT2 activation. *The Journal of Investigative Dermatology*, 133(3), 793–802.
- Karvonen, S. L., Korkiamäki, T., Ylä-Outinen, H., Nissinen, M., Teerikangas, H., Pummi, K., Karvonen, J., & Peltonen, J. (2000). Psoriasis and altered calcium metabolism: Downregulated capacitative calcium influx and defective calcium-mediated cell signaling in cultured psoriatic keratinocytes. *Journal of Investigative Dermatology*, 114(4), 693–700.
- Kawano, S., Otsu, K., Kuruma, A., Shoji, S., Yanagida, E., Muto, Y., Yoshikawa, F., Hirayama, Y., Mikoshiba, K., & Furuichi, T. (2006). ATP autocrine/paracrine signaling induces calcium oscillations and NFAT activation in human mesenchymal stem cells. *Cell Calcium*, 39(4), 313–324.
- Kobayashi, Y., Sanno, Y., Sakai, A., Sawabu, Y., Tsutsumi, M., Goto, M., Kitahata, H., Nakata, S., Kumamoto, J., Denda, M., & Nagayama, M. (2014). Mathematical modeling of calcium waves induced by mechanical stimulation in keratinocytes. *PLOS One*, 9(3), e92650.
- Koizumi, S., Fujishita, K., Inoue, K., Shigemoto-Mogami, Y., Tsuda, M., & Inoue, K. (2004). Ca²⁺ waves in keratinocytes are transmitted to sensory neurons: The involvement of extracellular ATP and P2Y2 receptor activation. *Biochemical Journal*, 380(2), 329–338.
- Korkiamaki, T., Yla-Outinen, H., Leinonen, P., Koivunen, J., & Peltonen, J. (2005). The effect of extracellular calcium concentration on calcium-mediated cell signaling in NF1 tumor suppressor-deficient keratinocytes. *Archives of Dermatological Research*, 296(10), 465–472.
- Kumai, M., Nishii, K., Nakamura, K. I., Takeda, N., Suzuki, M., & Shibata, Y. (2000). Loss of connexin45 causes a cushion defect in early cardiogenesis. *Development*, 127(16), 3501–3512.
- Lansdown, A. B., Sampson, B., & Rowe, A. (1999). Sequential changes in trace metal, metallothionein and calmodulin concentrations in healing skin wounds. *Journal of Anatomy*, 195(Pt 3Pt 3), 375–386.
- Leybaert, L., & Sanderson, M. J. (2012). Intercellular Ca(2+) waves: Mechanisms and function. *Physiological Reviews*, 92(3), 1359–1392.
- Liu, F., Putnam, A., & Jankowsky, E. (2008). ATP hydrolysis is required for DEAD-box protein recycling but not for duplex unwinding. *Proceedings of the National Academy of Sciences United States of America*, 105(51), 20209–20214.
- Martin, P. E., Easton, J. A., Hodgins, M. B., & Wright, C. S. (2014). Connexins: Sensors of epidermal integrity that are therapeutic targets. *FEBS Letters*, 588(8), 1304–1314.
- Mignen, O., Thompson, J. L., & Shuttleworth, T. J. (2001). Reciprocal regulation of capacitative and arachidonate-regulated noncapacitative Ca²⁺ entry pathways. *The Journal of Biological Chemistry*, 276(38), 35676–35683.
- Mignen, O., Thompson, J. L., & Shuttleworth, T. J. (2003). Calcineurin directs the reciprocal regulation of calcium entry pathways in nonexcitable cells. *The Journal of Biological Chemistry*, 278(41), 40088–40096.
- Moehring, F., Cowie, A. M., Menzel, A. D., Weyer, A. D., Grzybowski, M., Arzua, T., Geurts, A. M., Palygin, O., & Stucky, C. L. (2018). Keratinocytes mediate innocuous and noxious touch via ATP-P2X4 signaling. *eLife*, 7, 7.
- Ross, K., Whitaker, M., & Reynolds, N. J. (2007). Agonist-induced calcium entry correlates with STIM1 translocation. *Journal of Cellular Physiology*, 211(3), 569–576.
- Saez, J. C., Connor, J. A., Spray, D. C., & Bennett, M. V. L. (1989). Hepatocyte gap junctions are permeable to the second messenger, inositol 1,4,5-trisphosphate, and to calcium ions. *Proceedings of the National Academy of Sciences of the United States of America*, 86(8), 2708–2712.
- Sammak, P. J., Hinman, L. E., Tran, P. O., Sjaastad, M. D., & Machen, T. E. (1997). How do injured cells communicate with the surviving cell monolayer? *Journal of Cell Science*, 110(Pt 4), 465–475.
- Sneyd, J., Wetton, B. T., Charles, A. C., & Sanderson, M. J. (1995). Intercellular calcium waves mediated by diffusion of inositol trisphosphate: a two-dimensional model. *The American Journal of Physiology*, 268(6 Pt 1), C1537–C1545.
- Stathopoulos, P. B., Schindl, R., Fahrner, M., Zheng, L., Gasmı-Seabrook, G. M., Muik, M., Romanin, C., & Ikura, M. (2013). STIM1/Orai1 coiled-coil interplay in the regulation of store-operated calcium entry. *Nature Communications*, 4, 2963.
- Todd, C., & Reynolds, N. J. (1998). Up-regulation of p21WAF1 by phorbol ester and calcium in human keratinocytes through a protein kinase C-dependent pathway. *The American Journal of Pathology*, 153(1), 39–45.
- Tran, P. O., Hinman, L. E., Unger, G. M., & Sammak, P. J. (1999). A wound-induced [Ca²⁺]_i increase and its transcriptional activation of immediate early genes is important in the regulation of motility. *Experimental Cell Research*, 246(2), 319–326.
- Tsutsumi, M., Inoue, K., Denda, S., Ikeyama, K., Goto, M., & Denda, M. (2009). Mechanical-stimulation-evoked calcium waves in proliferating and differentiated human keratinocytes. *Cell Tissue Research*, 338(1), 99–106.
- Tu, C. L., Celli, A., Mauro, T., & Chang, W. (2019). Calcium-sensing receptor regulates epidermal intracellular Ca(2+) signaling and re-epithelialization after wounding. *The Journal of Investigative Dermatology*, 139(4), 919–929.
- Wilkins, B. J., Dai, Y. S., Bueno, O. F., Parsons, S. A., Xu, J., Plank, D. M., Jones, F., Kimball, T. R., & Molkenin, J. D. (2004). Calcineurin/NFAT coupling participates in pathological, but not physiological, cardiac hypertrophy. *Circulation Research*, 94(1), 110–118.
- Wilson Sarah, R., Thé, L., Batia Lyn, M., Beattie, K., Katibah George, E., McClain Shannan, P., Pellegrino, M., Estandian Daniel, M., Bautista, & Diana, M. (2013). The epithelial cell-derived atopic dermatitis cytokine TSLP activates neurons to induce itch. *Cell*, 155(2), 285–295.
- Xu, S., & Chisholm, A. D. (2011). A Gαq-Ca²⁺ signaling pathway promotes actin-mediated epidermal wound closure in *C. elegans*. *Current Biology*, 21(23), 1960–1967.
- Xue, S., Nicoud, M. R., Cui, J., & Jovin, D. J. A. (1994). High concentration of calcium ions in Golgi apparatus. *Cell Research*, 4(1), 97–108.
- Zhang, X., Gueguinou, M., & Trebak, M. (2018). Store-independent orai channels regulated by STIM. In J. A. Kozak, & J. W. Putney, Jr. (Eds.), *Calcium entry channels in non-excitable cells* (pp. 197–214). CRC Press/Taylor & Francis.

SUPPORTING INFORMATION

Additional Supporting Information may be found online in the supporting information tab for this article.

How to cite this article: Hudson, L., Begg, M., Wright, B., Cheek, T., Jahoda, C. A. B., & Reynolds, N. J. (2021). Dominant effect of gap junction communication in wound-induced calcium-wave, NFAT activation and wound closure in keratinocytes. *J Cell Physiol*, 236, 8171–8183. <https://doi.org/10.1002/jcp.30488>